의학박사 학위논문

Development of Allogeneic Hair Transplantation by Antigen-specific Immune Tolerance

항원 특이적 면역 관용을 통한 동종간 모발이식술 개발

2017년 8월

서울대학교 대학원

의학과 피부과학전공

김 진 용

Development of Allogeneic Hair Transplantation by Antigen-specific Immune Tolerance

항원 특이적 면역 관용을 통한 동종간 모발이식술 개발

지도교수 권 오 상

이 논문을 의학박사 학위논문으로 제출함
2017년 7월

서울대학교 대학원
의학과 피부과학전공
김 진 용

김 진 용의 박사학위논문을 인준함
2017년 5월

위 원 장 _____ (인)
부 위 원 장 _____ (인)
위 원 _____ (인)
위 원 _____ (인)
위 원 _____ (인)

Development of Allogeneic Hair Transplantation by Antigen-specific Immune Tolerance

by

Jin Yong Kim, M.D.

(Directed by Ohsang Kwon, M.D., Ph.D.)

A Thesis Submitted to the Department of Medicine
in Partial Fulfillment of the Requirements for the Degree
of Doctor of Philosophy in Medicine (Dermatology)
at the Seoul National University College of Medicine

July 2017

Approved by thesis committee

Chairman Professor KYU HAN KIM

Vice Chairman Professor Ohsang Kwon

Professor Kyeong Cheon Jung

Professor Jae Il Lee

Professor Dong Youn Lee

CONTENTS

ABSTRACT

Development of Allogeneic Hair Transplantation by Antigen-specific Immune Tolerance

Jin Yong Kim

Department of Dermatology, College of Medicine

The Graduate School Seoul National University

Severe permanent alopecia patients cannot benefit from autologous hair transplantation because of the shortage of donor hair follicles (HFs). Therefore, allogeneic hair transplantation is considered as an alternative option, but the generalized immunosuppression cannot be justified for the non-life-threatening disease. For the development of allogeneic hair transplantation with antigen-specific immune tolerance, the dendritic cell (DCs) is focused as a key target for tolerance induction. The alloantigen presentation by immature DCs or the depletion of donor resident DCs can be new immunomodulatory strategy for the prevention of rejection process. In this study, the tolerogenic potential of anti-ICAM1 antibody (MD-3) and the immunomodulatory effect of UVB pre-irradiation plus anti-CD154 antibody treatment was evaluated under the skin immune system in MHC-mismatched HF allograft model in nonhuman primates and humanized mouse.

In the first part, following the preparation of recipient sites with a hair-removing diode laser, donor HFs from monkey's thick eyebrow were transplanted into recipient back skin under the treatment of MD-3 antibody and short-term immunosuppressant (IS). The survival of HF allografts was significantly enhanced in MD-3 treatment group, whereas rapidly impaired in the immunosuppressant only and control groups. On histological examination, the outer root sheath of HF allograft was maintained over several weeks in the MD-3 treatment group, whereas rapidly destroyed in the control group. Although long-term survival was not achieved, MD-3 treatment markedly enhanced HF allograft survival by the delayed and diminished perifollicular T cell infiltration.

In the second part, humanized mice were generated by the infusion of human $CD34^+$ hematopoietic stem cells into NOD/Lt-scid IL2rγ null mice, then incubated for 16 weeks to repopulate the human immune system. UVB was pre-irradiated to donor HFs to make tissue resident donor DCs migrate out of donor tissue, and anti-CD154 antibody was treated to recipient humanized mice to block the maturation of recipient DCs and co-stimulatory signaling during direct and indirect antigen presentation pathway. Surprisingly, the long-term survival of HF allografts was achieved showing normal hair cycle with newly growing black pigmented hair shafts.

In the first part, anti-ICAM1 antibody combined with short-term rapamycin treatment enhanced the HF allograft survival in nonhuman primate model. This attempt efficiently suppressed alloreactive T cell

response, but only targeted to the recipient immune system. In the second part, we observed the long-term survival of HF allograft achieved under the UVB pre-irradiation to the donor HFs by significantly diminishing alloreactive T cell infiltration in humanized mouse model. In conclusion, the induction of antigen-specific T cell tolerance by MD-3 antibody or UVB pre-irradiation could be adopted in the skin immune system and these can be a potent immunomodulatory tool for preventing allograft rejection.

Keywords: allogeneic hair transplantation, alopecia, anti-CD154 antibody, anti-ICAM1 antibody, dendritic cell, hair transplantation, humanized mouse, immune tolerance, nonhuman primate, UVB irradiation

Student Number: 2013-21669

LIST OF FIGURES

INTRODUCTION

Permanent alopecia significantly affects body image, impairs self-esteem, and influences social and psychological behavior [1]. For the treatment of permanent alopecia, autologous hair transplantation (HTPL) has been considered as the effective treatment option. However, a patient with severe permanent alopecia cannot benefit from autologous HTPL because of the shortage of donor hair follicles (HFs). Especially, childhood cancer survivors after high-dose conditioning chemotherapy used to suffer from chemotherapy-induced permanent alopecia for their entire life [2]. In the clinical setting, parents may wish to donate some of their hair to their children. However, allogeneic HTPL cannot be successful without generalized immunosuppression, and the side effects of long-term immunosuppression cannot be justified for non-life-threatening diseases. Therefore, new immunomodulatory regimen is necessary for the success of allogeneic HTPL in severe permanent alopecia patients.

The induction of T cell tolerance to specific antigens has been attempted using dendritic cells (DCs) as key targets for tolerance induction [3]. Antigen presentation by immature or semi-mature DCs results in T cell tolerance because of the failure to provide sufficient co-stimulatory signals [4-6]. These tolerogenic DCs are characterized by low-level expression of surface major histocompatibility complex (MHC) molecules and co-stimulatory receptors and low-level production of

Th1 cytokines [5]. Otherwise, the immune recognition of alloantigen is complicated by the fact that both donor and recipient antigen presenting cells (APCs) can present donor antigens to recipient T cells. These pathways result in recipient T cells that can be restricted to either donor (direct pathway) or recipient (indirect pathway) MHC molecules. Among these, donor DCs in graft tissue play as a key role of antigen presentation with direct pathway displaying donor antigen molecules to recipient T cells [7]. Therefore, if the resident donor DCs can be depleted in donor tissue before transplantation, it could efficiently reduce the acute rejection by blocking the direct pathway.

Recently, MD-3 antibody was developed as an anti-human intercellular adhesion molecule 1 (ICAM-1) antibody cross-functional on nonhuman primates [8]. Antibody-mediated ligation of ICAM-1 arrests DCs in the semi-mature stage and induces specific T cell tolerance against grafted antigens rather than generalized immunosuppression. Previously, MD-3 treatment has been shown to achieve long-term xenograft survival in nonhuman primates when combined with low-dose rapamycin and anti-CD154 blocking antibody [8].

Ultraviolet (UV) radiation, especially UVB radiation (280-315nm), has suppression effects of cellular immunity in the skin immune system [9]. For example, natural killer cell activity is inhibited, antigen presentation is changed, and the development of T-helper 2-like immune responses is favorable [10]. UVB phototherapy is well known to decrease the number of epidermal T lymphocytes and DCs in the patients of inflammatory

skin disease [11]. Therefore, the depletion of DCs in donor tissue prior to transplantation can be a novel strategy for HF allograft to efficiently block the direct antigen presentation pathway.

In the first part, we evaluated the tolerogenic potential of MD-3 pre-treatment in MHC-mismatched HF allograft model in nonhuman primates. We prepared recipient sites with the diode laser on the monkey upper back skin. MD-3 antibody was introduced before transplantation and evaluated by dermoscopy, histology, immunohistochemistry for perifollicular inflammatory cell infiltrates, and ELISPOT assay and donor-specific antibody (DSA) formation. We observed that MD-3 significantly enhanced the HF allograft survival, regardless of the concomitant immunosuppressant therapy, by preferential impediment of alloreactive $CD3^+$ T cell infiltration.

Then, for the second part, we evaluated the tolerogenic potential of UVB pre-irradiation combined with anti-CD154 antibody in MHC-mismatched HF allograft model in humanized mice. UVB pre-irradiation was introduced to the donor HFs *in vivo* and *in vitro* and anti-human CD154 antibody was injected to the recipient humanized mice. The survival of HF allograft was evaluated by photography, histology, immunohistochemistry for perifollicular inflammatory cell infiltrates, and ELISPOT assay. We observed that UVB irradiation and/or anti-CD154 antibody achieved the long-term survival of HF allografts in humanized mice.

MATERIALS AND METHODS

PART 1.

Monkey and health monitoring

Sixteen Cynomolgus monkeys (*Macaca fascicularis*), weighing 3.6 to 5.0 kg (median body weight 4.4 kg), were maintained at the Non-Human Primate Center, Korea Institute of Toxicology. All Cynomolgus monkeys showed normal hematology and serum and urine chemistry, and tested negative for tuberculosis, Salmonella/Shigella, herpes B, simian T cell lymphotropic virus, simian immunodeficiency virus, simian retrovirus type D, hepatitis B, ectoparasites, and endoparasites. During the whole experiment, monkeys were regularly screened with respect to general symptoms, body weight, food and water intake, hematology, and serum and urine chemistry. All animal procedures were performed according to the American Association for the Accreditation of Laboratory Animal Care (AAALAC) guidelines and approved by the Institutional Animal Care and Use Committee, Korea Institute of Toxicology.

Laser hair removal

A 800nm diode laser (LightSheer XC system, USA) was tested on the monkey skin with multiple parameters of fluence (40 to 60 J/cm^2), pulse duration (30 to 100 ms), and repeat time (1 to 2 times). After 1 and 3

months, hair removal was checked with the dermoscopic and histological examinations. All monkeys were treated on the upper back skin with the parameter of 50 J/cm^2 x 30 ms x 2 times. All irradiations were performed with a fixed 9 mm square spot size and built in sapphire window contact cooling device under intramuscular ketamine anesthesia. Total 2 separate sessions were performed at 3 and 6 months prior to transplantation. Postoperatively, topical antibiotic was applied to the irradiated sites.

Hair transplantation

Sixteen Cynomolgus monkeys were randomly coupled to eight donor-recipient pairs and participated as a recipient and donor after screening of donor-specific antibody (DSA). Monkeys were divided into 3 groups and treated with MD-3 antibody plus short-term rapamycin (n=6, MD3+IS), short-term rapamycin only (n=5, IS), and none (n=5, Con). Donor hairs were harvested from the monkey eyebrow with strip incision, washed, and separated into HF units. Only eyebrow hairs were thick enough to be separated into follicular unit unlike body hairs. All grafts were kept in cooled (4° C) normal saline until needed, and transplanted into the recipient sites using the implanter [12]. For easy detection of HF allografts, donor hairs were implanted in the opposite direction of original hairs. As a result, each recipient monkey received total 19 to 65 HFs (mean 44.5 HFs) from the matched donor monkey. We performed photography, dermoscopy, and HF biopsies at 1, 2, and 4 weeks post-transplantation, and then observed every 4 weeks until 16 weeks. After

transplantation, recipient sites were covered with cotton gauzes and monkey jacket was put on for the prevention of plucking. All procedures were performed under intravascular zoletil anesthesia with lidocaine tumescent anesthesia in both donor and recipient sites.

Histology and immunohistochemistry

Formalin-fixed, paraffin-embedded tissues were sectioned at a thickness of 4 μm and stained with hematoxylin and eosin (H&E). For immunohistochemistry, tissue sections were dewaxed in xylene, rehydrated using a graded alcohol series, and incubated in an endogenous peroxide-blocking solution for 5 min. Antigen retrieval was performed by incubating the sections in target retrieval solution at 120° C for 10 min. Sections were blocked with pre-blocking solution (GBI Labs, USA) for 1 hr at room temperature, then incubated overnight at 4℃ with the primary antibodies diluted in the antibody diluent reagent solution buffer (Invitrogen, USA). After three washes with PBS, slides were incubated with secondary antibodies at room temperature for 1 hr. Then, sections were counterstained with hematoxylin (Dako, USA). Microscopic observations were performed with an Olympus Microscope BX43 Set equipped with DP70 camera (Olympus, Japan). We used cellSens software (Olympus, Japan) for image acquisition. The antibodies used were as follows: anti-CD3 (A0452, Dako, Denmark), anti-CD68 (clone KP1, Dako, USA), anti-CD4 (clone BC/1F6, abcam, UK), anti-CD8 (ab4055, abcam, UK), anti-A (Z2B-1, Santa Cruz, USA), anti-B (89-F,

Santa Cruz, USA), and anti-H (BRIC231, Santa Cruz, USA). The $CD3^+$ and $CD68^+$ positive cells distributed in the HFs and around a distance of the diameter of a hair bulb from HFs were counted using ImageJ (2-3 HPF/HF, 1-2 HFs/monkey) [13].

Detection of donor-specific antibody by flow cytometric analysis.

Donor peripheral blood (100 μl) was incubated with 100 μl of recipient sera for 30 min at 4° C after RBC lysis. Then, they were centrifuged and washed three times with cold PBS, followed by staining with FITC-labeled anti-human IgG antibodies (Santa Cruz, USA) that cross-react with Rhesus and Cynomolgus IgG. After washing with PBS and further staining with PerCP-conjugated anti-CD3 (Miltenyi Biotech, Germany) and phycoerythrin-conjugated anti-CD20 (Miltenyi Biotech, Germany), three-color flow cytometric analysis was performed with a FACSCalibur instrument (BD Biosciences, USA). Lymphocytes were gated on the basis of their forward and side-scatter characteristics, and DSA-positive population was quantified in $CD3^+$ T cells and $CD20^+$ B cells. Donor and multi-sensitized human sera were used as negative and positive control, respectively.

ELISPOT assay

The frequencies of IFN-γ-secreting antigen-specific T cells in peripheral blood of nonhuman primates were measured using an

ELISPOT kit (Mabtech®). Anti-IFN-γ capture antibody-coated plates were washed four times with sterile PBS (200 μl/well) and blocked for 30 min with 10% human serum-supplemented RPMI 1640 media at room temperature. After removing the media, 2.5×10^5 of PBMCs from recipient monkeys were cultured with 5×10^4 matched donor monkey cells in RPMI 1640 media supplemented with 10% human serum for 40 h at 37° C in a 5% CO2 incubator. As a negative control (-), recipient PBMCs were stimulated with none, and as a positive control (+), stimulated with anti-CD3 antibody. After the 40-h culture, cells were removed, and the plates were washed five times with PBS (200 μl/well). Alkaline phosphatase-conjugated detecting antibody diluted at 1:200 or 1:1,000 for IFN-γ in 100 μl PBS containing 0.5% fetal bovine serum was then added and incubated for 2 h at room temperature. The plates were washed five times with PBS, and 100 μl BCIP/NBP substrate was added. Color development was stopped by washing with tap water. The resulting spots were counted on a computer-assisted ELISPOT Reader System (AID).

Statistical analyses

Data are shown as mean ± SEM. All statistical analyses were performed by R (The R Foundation) and SPSS version 21 (IBM Corporation). Survival analysis was used for determining statistical significance of visible hair follicle allografts count. Two-way ANOVAs were used for determining statistical significance of perifollicular $CD3^+$ T

cells and $CD68^+$ macrophages infiltration. Statistical significance was accepted when p values were lower than 0.05.

PART 2.

Generation of human hematopoietic stem cell engrafted humanized mice

NSG (NOD.Cg-$Prkdc^{scid}Il2rg^{tm1Wjll}$/SzJ, 005557, The Jackson Laboratory) male mice housed into an autoclaved, filtered, ventilated housing device. Humanized mice were generated according to a previously described protocol [14]. Total 68 fresh 8 weeks old NSG mice were irradiated with 220 cGy whole body 137Cs gamma irradiator. Total 23 human umbilical cord blood were purified to highly enriched $hCD34^+$ hematopoietic stem cell (HSC) populations using magnetic sorting (Miltenyi Biotech, Germany), suspended in PBS at 1.5×10^5 $CD34^+$ cells/0.5 ml, then loaded a 1-cc tuberculin syringe. Human $CD34^+$ cells were injected into the lateral tail vein of irradiated NSG mice within 4 hours after gamma irradiation. NSG mice were allowed for human HSC to engraft in mice for over 12 weeks to 16 weeks. All animal procedures were performed according to the American Association for the Accreditation of Laboratory Animal Care (AAALAC) guidelines and approved by the Institutional Animal Care and Use Committee, Seoul National University (SNU-150212-5, SNU-150212-6).

Human immune cell analysis by flow cytometry

Repopulation of total human hematopoietic cells and T cells in peripheral blood was monitored at 12 and 16 weeks post-transplantation by flow cytometric analysis. Peripheral bloods from humanized mice (100 μl) were centrifuged and washed three times with cold PBS after RBC lysis. Then, they were incubated with fluorochrome-labeled monoclonal antibodies anti-human HLA-ABC (YG13, BD Biosciences, USA), CD14 (MEM-18, BD, USA), CD19 (HIB19, BD, USA), CD3 (UCHT1, BD, USA), CD4 (RPA-T4, BD, USA) for 30min at 4° C. Three-color flow cytometric analysis was performed with a FACSCalibur instrument (BD Biosciences, USA). Lymphocytes were gated on the basis of their forward and side-scatter characteristics, and positive population was quantified in $hHLA-ABC^+$ cells. At the time of sacrifice, spleens were collected, and single cells were re-suspended in flow cytometry buffer (PBS with 0.1% bovine serum albumin and 0.1% Na azide). After staining with fluorochrome-conjugated antibodies for 30min at 4° C, the live cells were analyzed using a flow cytometer.

Human hair follicle transplantation

Donor HFs were harvested from occipital scalp of human healthy volunteers with strip incision, washed, and separated into follicular units. HF grafts were kept in 4° C normal saline within 4 hours after UVB irradiation or not, and transplanted into the upper back skin of recipient mice using the implanter [12]. White-colored mouse hair shafts were

shaved locally with an electric shaver. For the prevention of pulling out of HF allografts, donor hairs were implanted in the upper 1/3 position of mouse back skin. Black-pigmented donor HFs were selected so that it is very easy to differentiate between transplanted human HFs and surrounding mouse HFs. All procedures were performed under isoflurane gas anesthesia with vaporizer and O_2 supplier. Anti-human CD154 antibody was injected to recipient humanized mice intraperitoneally (dosage 20mg/kg) at -7, -3, 0, 3, 7, 12, 17 days, then 3, 4, 5, 6, 7, 8, 10, 12 weeks post-transplantation. Each recipient mouse received total 40 human HFs in the upper back skin by follicular unit transplantation. We performed photography and biopsies at 3 days, 1, 2, 4 weeks post-transplantation, and then again every 4 weeks until 16 weeks. This study was approved by the Institutional Review Board at Seoul National University Hospital (IRB-1212-118-454) and conducted according to the approved protocol.

UVB irradiation to donor HFs *in vivo* and *in vitro*

A UVB irradiation device containing F75/85W/UV21 fluorescent sun lamps (Philips, Einthoven, Netherlands) with an emission spectrum between 275 and 380 nm were used as the UV source. The distribution of their power output was 56.7% UVB (280 – 320 nm), 42.8% UVA (320 – 400nm), and 0.5% UVC (<280 nm). A Kodacel filter (TA401/407, Kodak, Rochester, NY, USA) was mounted 2 cm in front of the UV lamp to remove wavelengths of less than 290 nm (UVC). The UV intensity was

measured using a UV photometer (Model 585100, Waldmann Co., Villingen-Schwenningen, Germany). First, a minimal erythema dose was measured and the sub-erythema dose (0.9 MED) was irradiated to the half of shaved scalp *in vivo* 3 days before transplantation. Then, minimal harmful dose (50mJ/cm^2) was re-irradiated to the follicular unit of donor HFs *in vitro* 2 hours before transplantation.

Histology, immunohistochemistry and immunofluorescence

Formalin-fixed, paraffin-embedded tissues were sectioned at a thickness of 4 μm and stained with hematoxylin and eosin (H&E). For immunohistochemistry, tissue sections were dewaxed in xylene, rehydrated using a graded alcohol series, and incubated in an endogenous peroxide-blocking solution for 5 min. Antigen retrieval was performed by incubating the sections in target retrieval solution at 120° C for 5 min. Sections were blocked with pre-blocking solution (GBI Labs, USA) for 30 min at room temperature, then incubated overnight at 4℃ with the primary antibodies diluted in the antibody diluent reagent solution buffer (Invitrogen, USA): anti-hCD3 (A0452, Dako, Denmark), anti-hHLA-DP,DQ,DR (MHC class II, M0775, Dako, Denmark), anti-hHLA-ABC (MHC class I, SC-25619, Santa cruz, USA). After three washes with PBS, slides were incubated with secondary antibodies at room temperature for 1 hour. Then, sections were counterstained with hematoxylin (Dako, Denmark).

For immunofluorescence, frozen tissues were sectioned at a thickness of 4 μm and incubated with primary antibodies diluted in the antibody diluent reagent solution buffer (Invitrogen, USA) for 3 hours: anti-hHLA-DP,DQ,DR (MHC class II, M0775, Dako, Denmark), anti-hCD1a (M0721, Dako, Denmark), anti-hCD11c (3.9, BioLegend, United Kingdom), anti-p53 (DO7, NCL-L-p53-DO7, Novocastra, United Kingdom). After three washes with PBS, slides were incubated with secondary antibodies Alexa-Fluor 488-labeled goat anti-mouse IgG antibodies (polyclonal, ThermoFisher, USA) for 1 hour. The nuclei were counterstained with 4',6-diamidino-2-phenylindole (DAPI). For TUNEL stain, frozen tissues were stained with ApopTag® Fluorescein In Situ Apoptosis Detection Kit (S7110, Merck Millipore, Germany) according to the manufacturer's protocol.

Microscopic observations were performed with an Olympus Microscope BX43 Set equipped with DP70 camera (Olympus, Japan). We used cellSens software (Olympus, Japan) for image acquisition. Immunofluorescence was observed and captured using Leica fluorescence microscope (Leica Microsystems, Germany). The positively stained cells distributed in the HFs and around a distance of the diameter of a hair bulb from HFs were counted using ImageJ (3 fields/HF, 3-4 HFs/group).

ELISPOT assay

The frequencies of IFN-γ-secreting antigen-specific T cells in spleens of humanized mice were measured using an ELISPOT kit

(Mabtech, Sweden). Anti-IFN-γ capture antibody-coated plates were washed four times with PBS (200 μl/well) and blocked for 30 min with 10% human serum-supplemented RPMI 1640 media at room temperature. After removing the media, 3×10^5 recipient splenocytes from humanized mice were cultured with 5×10^4 donor PBMCs from human healthy volunteers in RPMI 1640 media supplemented with 10% human serum for 40 hours at 37° C in a 5% CO2 incubator. As a negative control, recipient splenocytes were stimulated with none, and as a positive control, stimulated with third-party γ-irradiated human PBMCs, and as a human T cell control, stimulated with anti-human CD3 antibody. After the 40 hours culture, cells were removed, and the plates were washed five times with PBS (200 μl/well). Alkaline phosphatase-conjugated detecting antibody diluted at 1:1,000 for IFN-γ in 100μl PBS containing 0.5% fetal bovine serum was then added and incubated for 2 hours at room temperature. The plates were washed five times with PBS, and 100μl BCIP/NBP substrate was added. Color development was stopped by washing with tap water. The resulting spots were counted on a computer-assisted ELISPOT Reader System (AID).

Statistical analyses

Data are shown as mean+/-SEM. All statistical analyses were performed by SPSS version 21 (IBM Corporation, USA). Student's t test were used for determining statistical significance. Statistical significance was accepted when p values were lower than 0.05.

RESULTS

PART 1. Allogeneic Hair Transplantation with Enhanced Survival by Anti-ICAM-1 Antibody with Short-term Rapamycin Treatment in Nonhuman Primates

Hair removal of monkey upper back skin with a diode laser

Before the hair transplantation, we prepared recipient sites on the upper back skin to prevent plucking of the transplanted HFs. Similar to the Japanese monkey [15], the Cynomolgus monkey is covered with melanin-rich medullated hair and melanin-poor unmedullated hair having different diameters (Fig. 1-1ab). Using a diode laser, the medullated hair was targeted and we aimed to destroy the unmedullated hair simultaneously [16]. After the test session for hair removal, we determined the appropriate parameter of 50 J/cm^2 x 30 ms x 2 times. Monkey hairs were efficiently removed with initial mild ulceration (Fig. 1-1cd). After 1 to 2 weeks, irradiated sites recovered well with dense collagen bundles and abundant melanophages in the dermis (Fig. 1-1ef). The recipient sites of each monkey were treated at two separate time points; 3 and 6 months prior to transplantation.

The survival of HF allografts was enhanced by MD-3 treatment

Sixteen Cynomolgus monkeys were randomly coupled to eight donor-recipient pairs and participated as a recipient and donor after screening of DSA. Monkeys were divided into three groups (Fig. 1-3a) and treated with the MD-3 antibody plus short-term low-dose rapamycin (n=6, MD3+IS), short-term low-dose rapamycin only (n=5, IS), or no treatment (n=5, Con). MD-3 was injected twice (dosage 8 mg/kg) intravenously at 1 and 4 days before transplantation. Low-dose rapamycin (trough level 6-12 μg/mL) was administered for only 3 weeks. Eyebrow HFs of the donor monkey were transplanted into the upper back skin of the recipient monkey by follicular unit transplantation (Fig. 1-2). As a result, each recipient monkey received total 20 to 61 HFs from the matched donor monkey. We performed dermoscopy, and biopsies at 1, 2, and 4 weeks post-transplantation, and then again every 4 weeks until 16 weeks. The survival of visible HF allografts was maintained in the MD3+IS group (p<0.0001), but was rapidly decreased in the IS (p=0.0251) and Con groups (Fig. 1-3bc).

The difference between the MD3+IS and other groups was obvious on dermoscopic examination (Fig. 1-4a). To confirm the survival of HF allografts, the intactness of the outer root sheath (ORS) was examined on histological examination (Fig. 1-4b). At 1 week, the ORS in the MD3+IS group maintained with an orderly structure, whereas those in the IS and Con groups showed destruction with inflammation. At 2 weeks, the ORS was intact only in the MD3+IS group, whereas destroyed in other groups. HFs were shrunk with prominent inflammatory cell

infiltration in the IS group. Massive granulomatous inflammation was found to replace the destroyed HFs in the Con group. The ORS in the MD3+IS group appeared shrunk at 4 weeks. Thus, we concluded that MD-3 pretreatment failed to achieve long-term graft survival, but remarkably enhanced allograft survival.

For the differentiation of HF allograft from the recipient's HFs, we performed immunohistochemical staining of ABO blood group antigens. ABO antigens were discovered in red blood cells and blood vessels, also in the epidermis, hair shaft, and matrix cells in human [17, 18]. In Cynomolgus monkey, human-type ABO antigens are not detected in red blood cells but they are present in the saliva and serum antibodies [17]. Interestingly, we found that ABO antigens were also expressed in blood vessels and epidermis of Cynomolgus monkey. The ORS of HF allografts showed positive staining according to the ABO group of the donor monkey, whereas the surrounding dermal blood vessels expressed ABO antigen of the recipient monkey (Fig. 1-5).

$CD3^+$ T cell infiltration was delayed and diminished under MD-3 treatment

To evaluate the immunological effect of MD-3 treatment, we assessed the perifollicular inflammatory cell infiltration by quantitative immunohistochemistry. Using the image analysis, perifollicular $CD3^+$ and $CD68^+$ cells were counted as previously reported [13, 19]. In the MD3+IS group, the infiltration of $CD3^+$ cells was significantly delayed, and the

total number was lower than other groups (Fig. 1-6a, $p < 0.0001$, between groups and time points). However, perifollicular $CD68^+$ cell infiltrates were already increased at 1 week and were similar between groups (Fig. 1-6b). Thus, MD-3 pretreatment impaired the perifollicular $CD3^+$ T cell response, regardless of concomitant rapamycin therapy. Without MD-3 or immunosuppressant therapy, HF allografts were substituted with heavy aggregation of $CD3^+$ T cells and $CD68^+$ macrophages resulting in a foreign body granuloma. Notably, most $CD3^+$ T cells were $CD8^+$ cytotoxic T cells in all groups (Fig. 1-6c).

Interferon (IFN)-γ-secreting T cells were significantly increased after hair follicle allograft in the IS and Con groups ($p=0.0131$), and no recipient monkeys produced DSAs regardless of the termination of rapamycin therapy (Fig. 1-7). We concluded that cellular rejection was the major rejection mechanism in HF allograft model than humoral rejection.

PART 2. Long-term survival of HF allografts was achieved by UVB pre-irradiation and anti-CD154 antibody treatments in humanized mice.

Generation of humanized mice with $CD34^+$ human hematopoietic stem cells

For the generation of humanized mice, we used NSG (NOD.Cg-Prkdc^{scid}Il2rg^{tm1Wjll}/SzJ, 005557, The Jackson Laboratory) immunodeficient mouse strains [20]. Total 23 human umbilical cord blood were purified to highly enriched human CD34$^+$ hematopoietic stem cell (HSC) populations. Total 68 NSG mice were irradiated with 220 cGy whole body ^{137}Cs gamma irradiator, then 1.5-2.0$\times10^5$ CD34$^+$ cells/mouse was injected into the mouse tail vein within 4 hours after gamma irradiation [14]. Then, human cell populations were analyzed with the surface marker of human HLA-ABC, CD14, CD19, CD3 from the peripheral blood of HSC-injected mice (Figure 2-1a). Human HLA-ABC$^+$ cells were successfully detected and grown until 16 weeks post-transplantation (Figure 2-1b, hHLA-ABC, $p<0.0001$, 12W 7.01±1.02%, 16W 13.9±2.18%). Human CD14$^+$ monocytes and CD19$^+$ B cells were repopulated earlier than CD3$^+$ T cells at 12 weeks post-transplantation (hCD14, $p<0.0001$, 12W 0.31±0.04%, 16W 1.37±0.17%; hCD19, $p=0.107$, 12W 3.29±0.71%, 16W 9.47±2.00%). To obtain sufficient volume of CD3$^+$ T cell population, HSC-injected mice were incubated for additional 4 weeks (hCD3, $p=0.0064$, 12W 0.68±0.24%, 16W 1.86±0.55%). Finally, we sorted out 24 successfully humanized mice with the criteria of over 1% HLA-ABC$^+$CD3$^+$ T cells in the peripheral blood (Figure 2-1c, hCD3, 3.18±2.42%) at 16 weeks post-transplantation.

Donor DCs were depleted by UVB pre-irradiation without apoptosis

UVB irradiation was known to make epidermal Langerhans cells migrate out of UVB-exposed skin to the draining lymph nodes, not by apoptosis [9, 21]. Based on these, UVB protocol was designed as the twice pre-irradiation to donor HFs when *in vivo* scalp state (dosage 0.9 MED) and *in vitro* follicular unit state (dosage 50mJ/cm^2) 3 days and 4 hours before transplantation, respectively [22-24]. To confirm the depletion of donor-derived DCs in HFs, UVB-irradiated HFs was evaluated by immunofluorescence of human MHC class II, CD1a, and CD11c. The number of DCs showed a significant decline in the ORS of UVB-irradiated HFs compared to unirradiated HFs (Figure 2-2a, $p<0.001$, n=6-10 HFs each group). Meanwhile, DC was not detected in the bulb area of HFs, consistent with the previous report [25]. Since UVB irradiation is a major environmental hazard inducing apoptosis to keratinocytes [23], apoptotic cell death was investigated by p53 and TUNEL staining. However, there is no significant change of the number of apoptotic cell between the UVB-irradiated and unirradiated HFs by our protocol (Figure 2-2b, n=8 HFs each group).

Long-term survival of HF allografts was achieved showing subsequent hair cycle

Non-humanized NSG mice were included for the elimination of bystander bias from xenogeneic innate immune response to human tissue (n=6, Group 1 NSG Con). Humanized mice were divided into 4 groups according to the treatment regimens as UVB pre-irradiation plus anti-CD154 antibody (Figure 2-3a; n=6, Group 2 HM UV+Ab), anti-CD154 antibody only (n=6, Group 3 HM Ab), UVB pre-irradiation only (n=6, Group 4 HM UV), and no treatment (n=6, Group 5 HM Con). UVB was pre-irradiated twice and anti-CD154 antibody was injected to recipient humanized mice intraperitoneally (dosage 20mg/kg) as the schedule shown in Figure 2-3b. Each recipient mouse received total 40 human HFs in the upper back skin by follicular unit transplantation. We performed photography and biopsies at 3 days, 1, 2, 4 weeks post-transplantation, and then again every 4 weeks until 16 weeks.

The surviving HF allografts were maintained in Group 2, 3, and 4 (Figure 2-3c, $p<0.0001$), but rapidly diminished in Group 5 within 3 weeks. The initial decrease of HF allografts due to plucking or movement was also observed in Group 1, rather than immunological effects (Figure 2-3d). Strikingly, the long-term survival of HF allografts was achieved in Group 2, 3, and 4 at 3 months post-transplantation, whereas there was no survived HF allograft in Group 5 (Figure 2-4a). The HF allografts showed newly growing black-pigmented shafts with anagen hair cycle until 6 months post-transplantation.

On histological examination, the ORS of HF allografts was maintained with an orderly structure as expected in Group 2, 3, and 4 (Figure 2-4b).

However, the ORS of HF allografts in Group 5 was destroyed with perifollicular inflammation and replaced with massive granulomatous inflammation. Notably, there were un-ignorable cellular infiltrations of small-sized mouse cells beside large-sized human immune cells around HF allografts. These small-sized mouse cells were also observed in Group 1. Taken together, we concluded that the combined treatment of UVB pre-irradiation and anti-CD154 antibody achieved the best survival result, but the single treatment of UVB pre-irradiation or anti-CD154 antibody also achieved the long-term survival of HF allograft.

$CD3^+$ T cell and MHC class II^+ macrophage infiltration was diminished under UVB pre-irradiation and anti-CD154 antibody treatment

To evaluate the immunological effect of UVB pre-irradiation and/or anti-CD154 antibody treatment, the perifollicular inflammatory cell infiltration was assessed by immunohistochemistry. Using the image analysis, perifollicular human $CD3^+$ T cells and MHC class II^+ macrophages were counted as previously reported [13, 19, 25]. Remarkably, the timing and amount of $CD3^+$ T cell infiltration was significantly delayed and reduced in Group 2, 3, and 4 compared to Group 5 (Figure 2-5a). However, the $CD3^+$ T cell infiltration was significantly increased at 1 week and persisted as inflammatory aggregation in Group 5. At 4 weeks, $CD3^+$ T cells were observed around HF allografts in Group 3 and 4, but still not observed in Group 2, correlated with the best survival of

Group 2. In the other hands, the amount of macrophage infiltration was significantly lower in the UV-treated Group 2 and 4 than the Ab only-treated Group 3 (Figure 2-5b). However, the infiltration of macrophage was significantly increased at 1 week and persisted in Group 5. In conclusion, alloreactive T cell and macrophage response were significantly suppressed by the UVB pre-irradiation regardless of the concomitant anti-154 antibody treatment.

UVB pre-irradiation alone did not induce antigen-specific T cell tolerance

To assess whether the transplanted animals developed antigen-specific T cell tolerance against to donor HFs, total splenocytes from humanized mice were stimulated with none (recipient), donor PBMCs (donor), and third-party γ-irradiated human PBMCs (third), and then ELISPOT assay was performed. The ELISPOT results was normalized to anti-human CD3 antibody reactive T cells to match the number of total human T cell in each group. When recipient humanized mice were sacrificed at 24 weeks post-transplantation, human HLA-ABC^{+} cells were still observed and well repopulated in total splenocytes of humanized mice (Figure 2-6a, 7.90$\pm$0.67%). Interestingly, the number of IFN-γ-secreting T cells against to donor antigens was much lower in the Ab-treated Group 2 and 3 than the UV only-treated Group 4 (Figure 2-6b, n=1 for each group). Therefore, we concluded that the long-term survival of HF allografts was not mediated by antigen-specific

T cell tolerance in the UV only-treated Group 4, while the suppression of T cell activity was shown in the Ab-treated Group 2 and 3.

Immune privilege was maintained in surviving HF allografts.

HFs are a unique site of immune privilege characterized by downregulation of MHC class I and expression of potent immunosuppressants [13]. The cells of the HF are protected against $CD8^+$ cytotoxic T lymphocyte attack similar to the cells in the anterior chamber of the eye [26]. Therefore, the status of immune privilege was evaluated to confirm whether the long-term survival is attributed to the immune privilege in the UV only-treated Group 4 (Figure 2-7). In the control Group 5, the ORS of HF allografts showed MHC class I expression already at 3 day and significantly higher expression at 4 weeks post-transplantation, likely to the damaging HFs in autoimmune disease [13]. But interestingly, the ORS of HF allografts maintained no MHC class I expression in Group 1, 2, 3 and the UV only-treated Group 4, showing the maintenance of HF immune privilege.

FIGURES

PART 1.

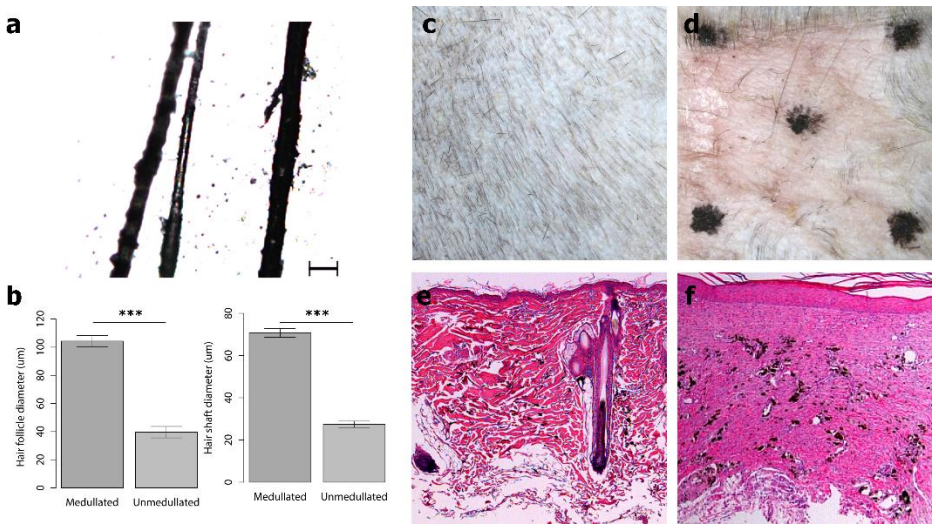

Figure 1-1. Hair characteristics and laser hair removal of Cynomolgus monkey

(a) Representative microscopic images of Cynomolgus monkey's hair shafts. Cynomolgus monkey is covered with medullated hair and unmedullated hair having (b) different hair follicle and shaft diameters (light, x40). Photographs of (c) upper back skin of the monkey and (d) after laser hair removal. Representative microscopic images of (e) upper back skin of the monkey and (f) after laser hair removal. (hematoxylin & eosin, x100).

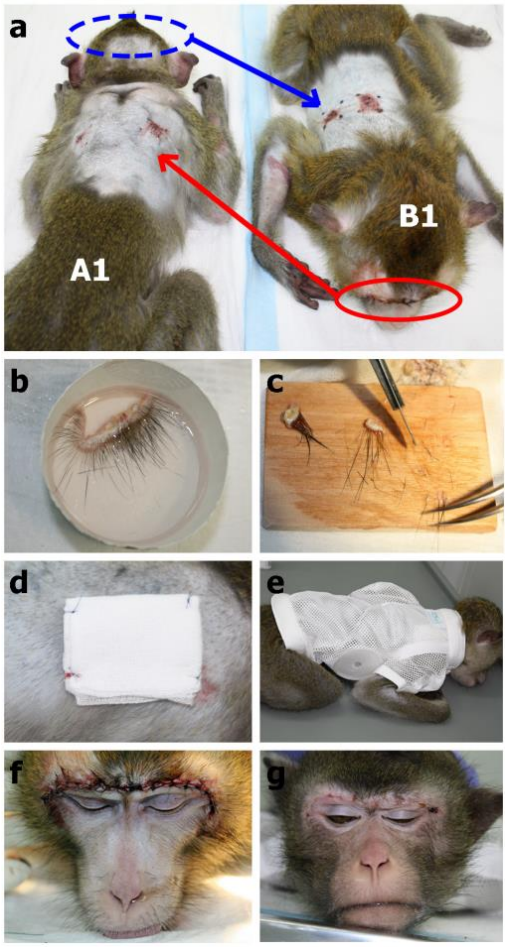

Figure 1-2. Hair follicle allograft model in nonhuman primates for transplantation research

(a) Sixteen Cynomolgus monkeys were randomly coupled to eight donor-recipient pairs and participated as a recipient and donor. (b) Donor eyebrow hairs were totally harvested as a strip incision and (c) separated into individual hair follicle units. (d) After transplantation, recipient sites were covered with cotton gauze and (e) a monkey jacket was put on for prevention of plucking. (f) Whole eyebrows were excised and sutured immediately and (g) completely recovered after 1 to 2 weeks.

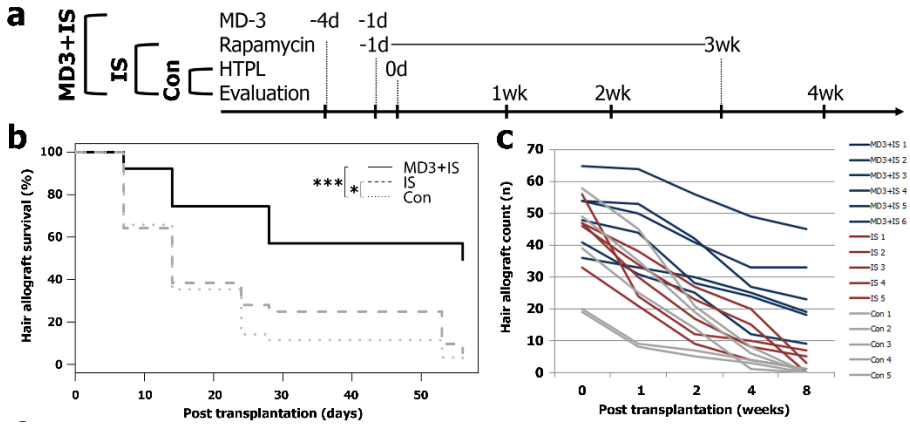

Figure 1-3. HF allograft survival was significantly enhanced under MD-3 therapy

(a) The experimental design is shown. Monkeys were divided into three groups and treated with MD-3 pretreatment plus short-term rapamycin (p<0.0001, n = 6, MD3+IS), short-term rapamycin only (p=0.0251, n = 5, IS), or no treatment (n = 5, Con). (b) The survival of visible hair follicle (HF) allografts in the MD3+IS, IS, and Con groups. (c) Number of visible HF allografts for each monkey. The MD3+IS group is shown as blue lines; the IS group is shown as red lines; and the Con group is shown as gray lines.

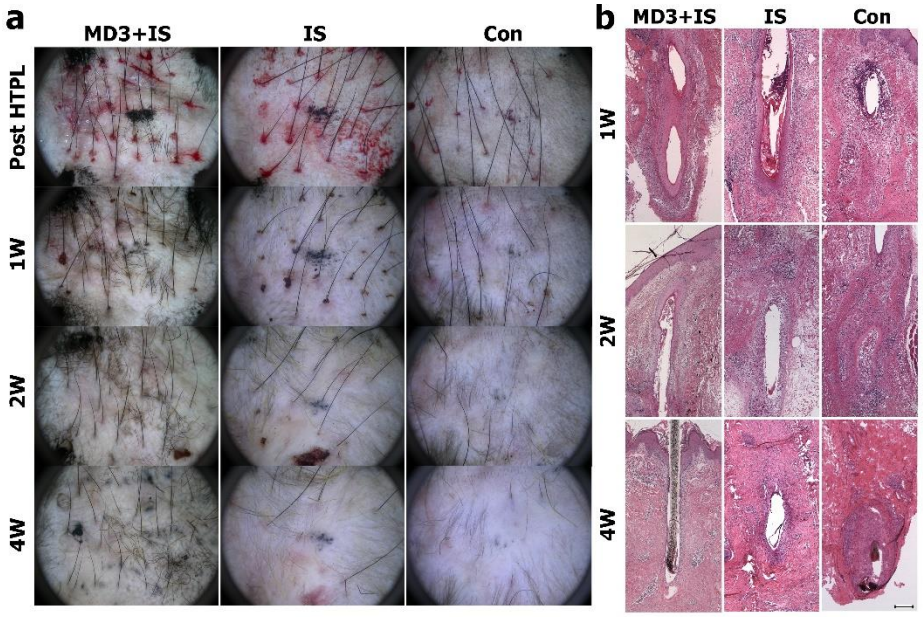

Figure 1-4. MD-3 antibody enhanced HF allograft survival in nonhuman primates

(a) Representative dermoscopic images from the three groups until 4 weeks after transplantation. (b) Representative microscopic images from the three groups until 4 weeks after transplantation. H&E staining is shown (hematoxylin & eosin; scale bar = 200 μm). HTPL, hair transplantation.

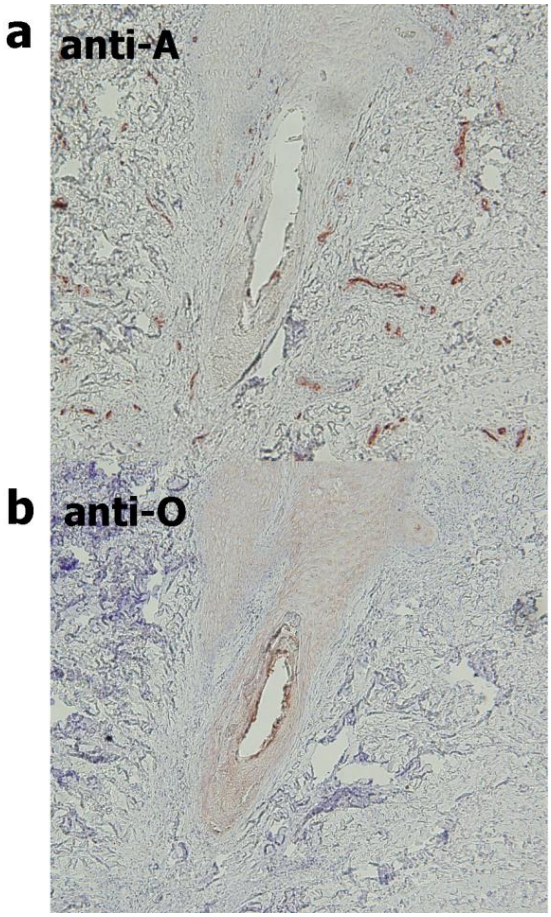

Figure 1-5. Identification of the allografted hair follicle from the recipient's own hair follicle

(a) While the surrounding dermal vessels showed positive staining according to the original ABO group of the recipient monkey, (b) the ORS of hair follicle allografts was stained as that in the donor monkey (immunoperoxidase, x100).

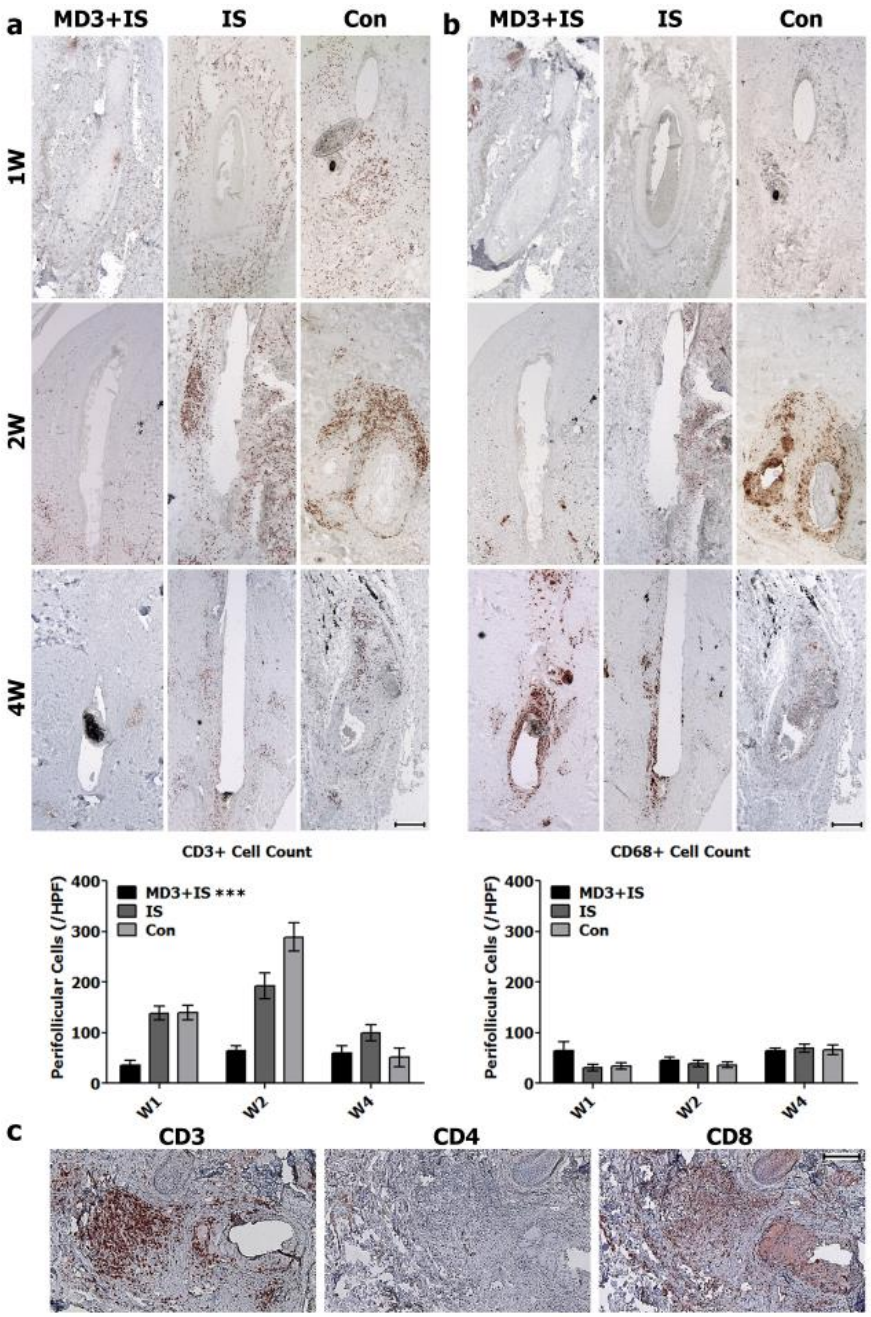

Figure 1-6. $CD3^+$ T-cell infiltration was delayed and reduced with MD-3 antibody treatment.

Representative microscopic images of immunohistochemistry results and quantification of perifollicular (a) $CD3^+$ T cells and (b) $CD68^+$ macrophages in

the MD3+IS, IS, and Con groups at 1, 2, and 4 weeks (2－3 HPF/HF, 1－2 HFs/monkey, immunoperoxidase; scale bar = 200 μm). (c) The T-cell-mediated cellular mechanism was the major rejection mechanism in the HF allografts (immunoperoxidase; scale bar = 200 μm). HF, hair follicle; HPF, high power field.

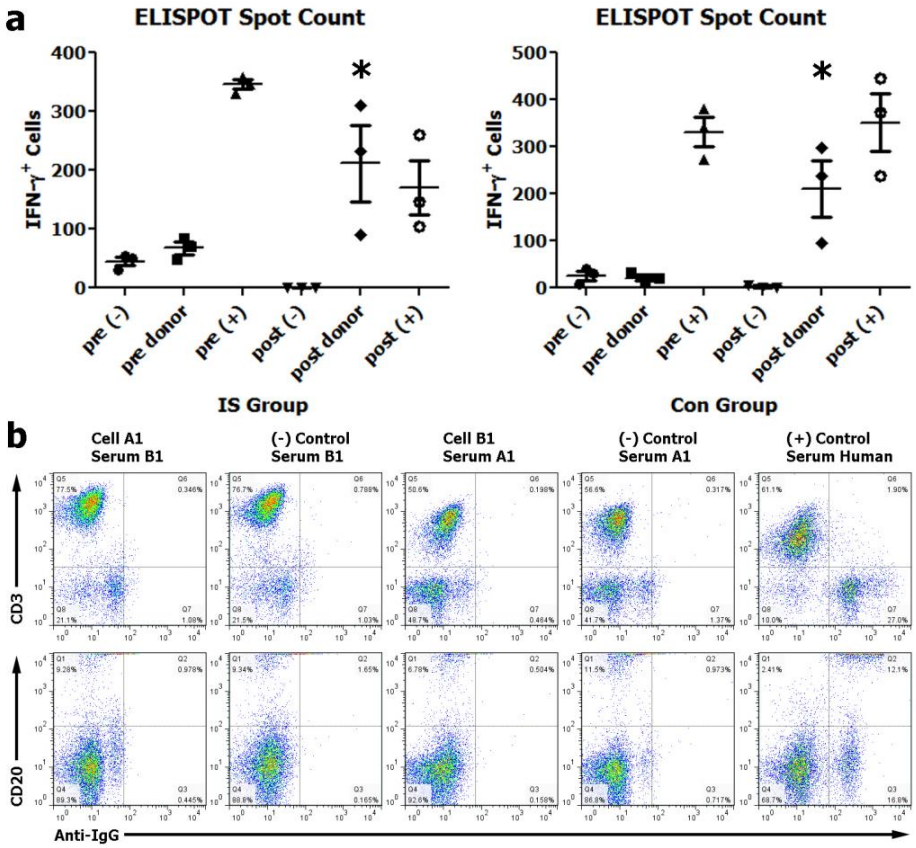

Figure 1-7. Hair follicle allografts were rejected by T-cell mediated rejection mechanism without donor-specific antibody formation

(a) Summarized data from ELISPOT assay to evaluate of IFN-γ secreting T cells in recipient PBMC stimulated with donor monkey cells. IFN-γ secreting T cells were significantly increased after hair follicle allografts both in IS and Con group (p=0.0131). (b) Representative flow cytometry plots of donor-specific antibody detection stained with PerCP-CD3, PE-CD20, and FITC-IgG antibodies. Donor lymphocytes were incubated with recipient sera corresponding donor-recipient pairs using PFC. None of the ten monkeys in all 3 groups developed DSAs.

PART 2.

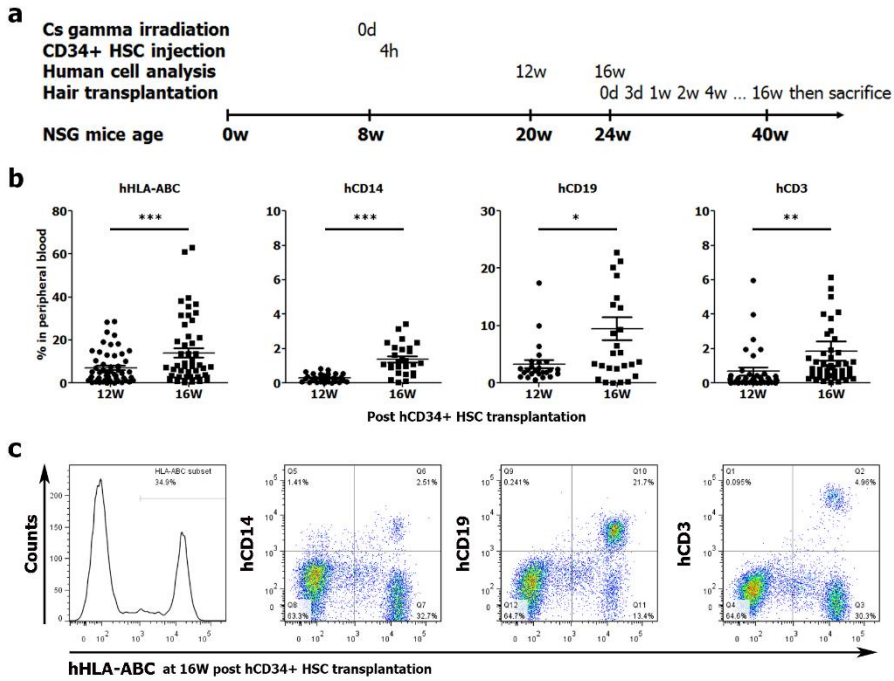

Figure 2-1. Generation of Hu-HSC humanized mice and human immune cell analysis

(a) The schedule for generation of Hu-HSC humanized mice and experimental design is presented. Total 68 NSG mice were irradiated with gamma irradiator, then 1.5-2.0×10^5 human $CD34^+$ cells/mouse was injected within 4 hours after Cs gamma irradiation. (b) Summarized data from flow cytometry analysis with the surface marker of human HLA-ABC, CD14, CD19, CD3 from the peripheral blood of humanized mice. Human $HLA-ABC^+$ cells were successfully repopulated until 16 weeks post-transplantation (hHLA-ABC, p<0.0001, 12W 7.01±1.02%, 16W 13.9±2.18%). (c) Representative flow cytometry plots of $hHLA-ABC^+$ cells in the peripheral blood of humanized mice at 16 weeks post-transplantation. *** $p < 0.001$, ** $p < 0.01$, * $p < 0.05$.

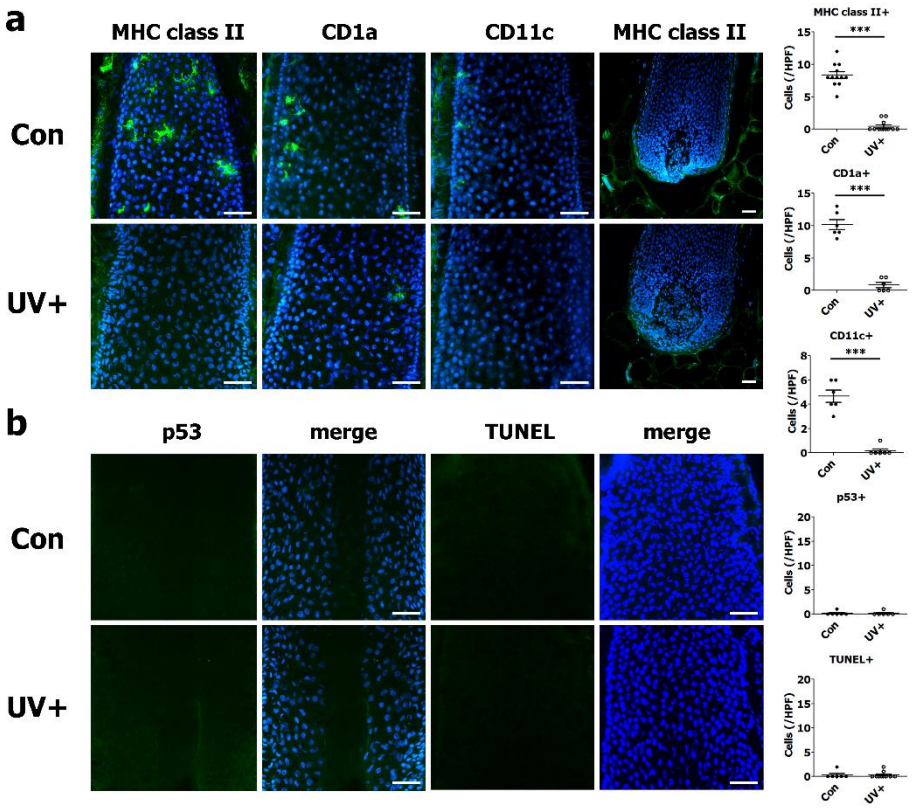

Figure 2-2. UVB pre-irradiation depleted donor-derived DCs in HFs.

(a) Representative immunofluorescence images of human MHC class II, CD1a, and CD11c for the detection of donor-derived DCs in unirradiated and UVB-irradiated HFs. After two sessions of UVB irradiation *in vivo* and *in vitro*, DCs were almost depleted in the ORS of donor HFs ($p<0.001$, n=6-10 HFs each group). (b) Representative immunofluorescence images of p53 and TUNEL staining for the detection of apoptotic cell death in unirradiated and UVB-irradiated HFs. The number of apoptotic cell was not different after two sessions of UVB irradiation (n=8 HFs each group, immunofluorescence, scale bar = 100 μm). *** $p < 0.001$.

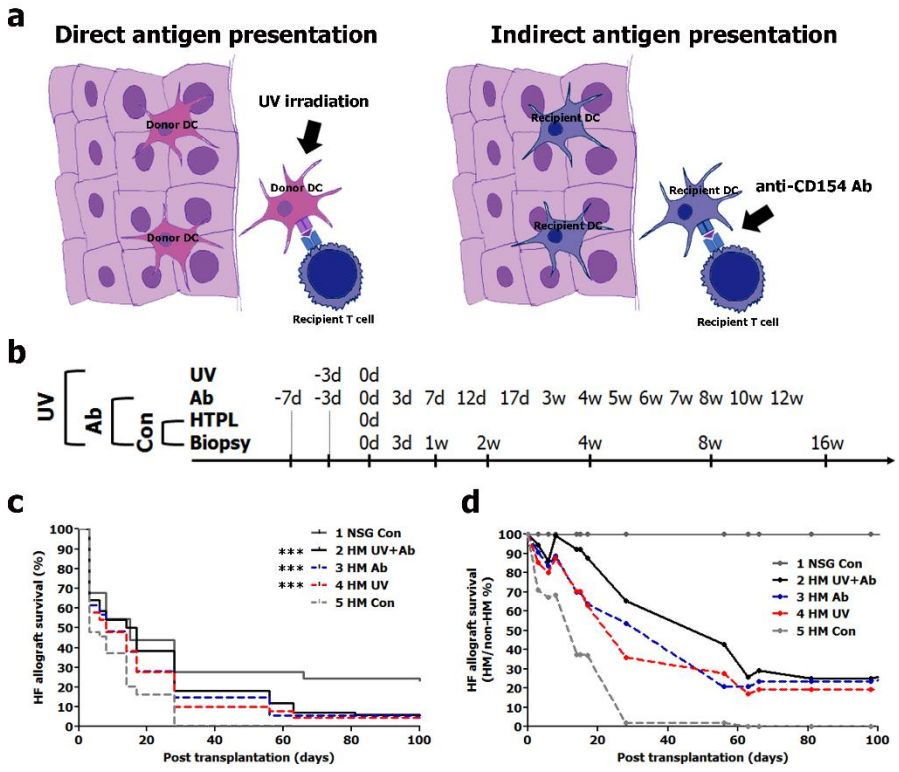

Figure 2-3. Long-term survival of HF allografts was achieved under UVB pre-irradiation and/or anti-CD154 antibody treatments.

(a) The dual blocking strategy targeting both antigen presentation process by donor DCs or recipient DCs. (b) HF allograft experimental design. NSG mice were included without humanized immune system (n=6, Group 1 NSG Con). Humanized mice were divided into 4 groups according to the treatment regimens as UVB pre-irradiation plus anti-CD154 antibody (n=6, Group 2 HM UV+Ab), anti-CD154 antibody only (n=6, Group 3 HM Ab), UVB pre-irradiation only (n=6, Group 4 HM UV), and no treatment (n=6, Group 5 HM Con). (c) The survival curve of HF allograft. (d) The relative survival curve of HF allograft in humanized mice group (Group 2-5) to non-humanized mice group (Group 1). The surviving HF allografts were observed in Group 2, 3, and 4 ($p<0.0001$), but rapidly diminished in Group 5.

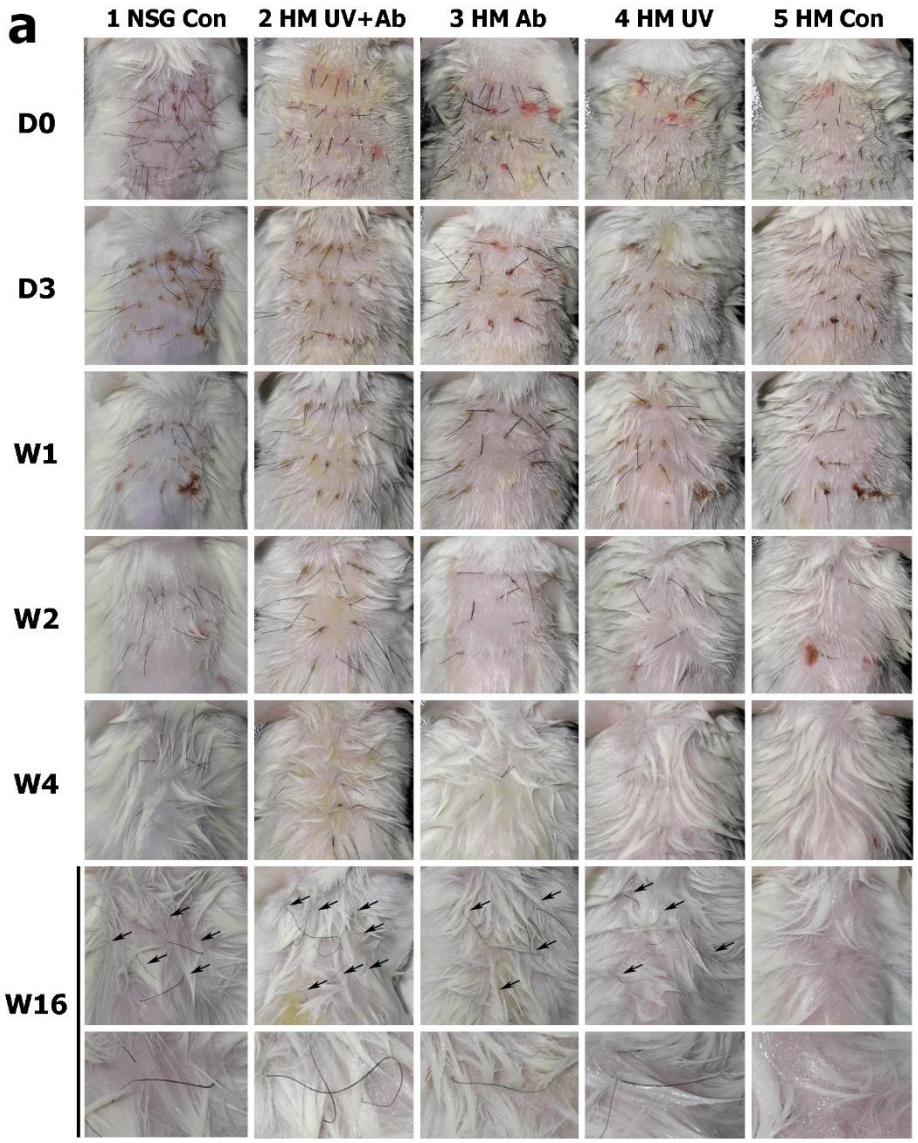

Figure 2-4. UVB pre-irradiation alone achieved HF allograft long-term survival in humanized mice.

(a) Representative photographs from Group 1-5 at 0 day, 3 days, 1 week, 2 weeks, 4 weeks, 16 weeks post-transplantation. The long-term survival of HF allografts was achieved showing newly growing black-pigmented shafts in Group 2, 3, and 4 at 3 months post-transplantation, whereas there was no survived HF allograft in Group 5.

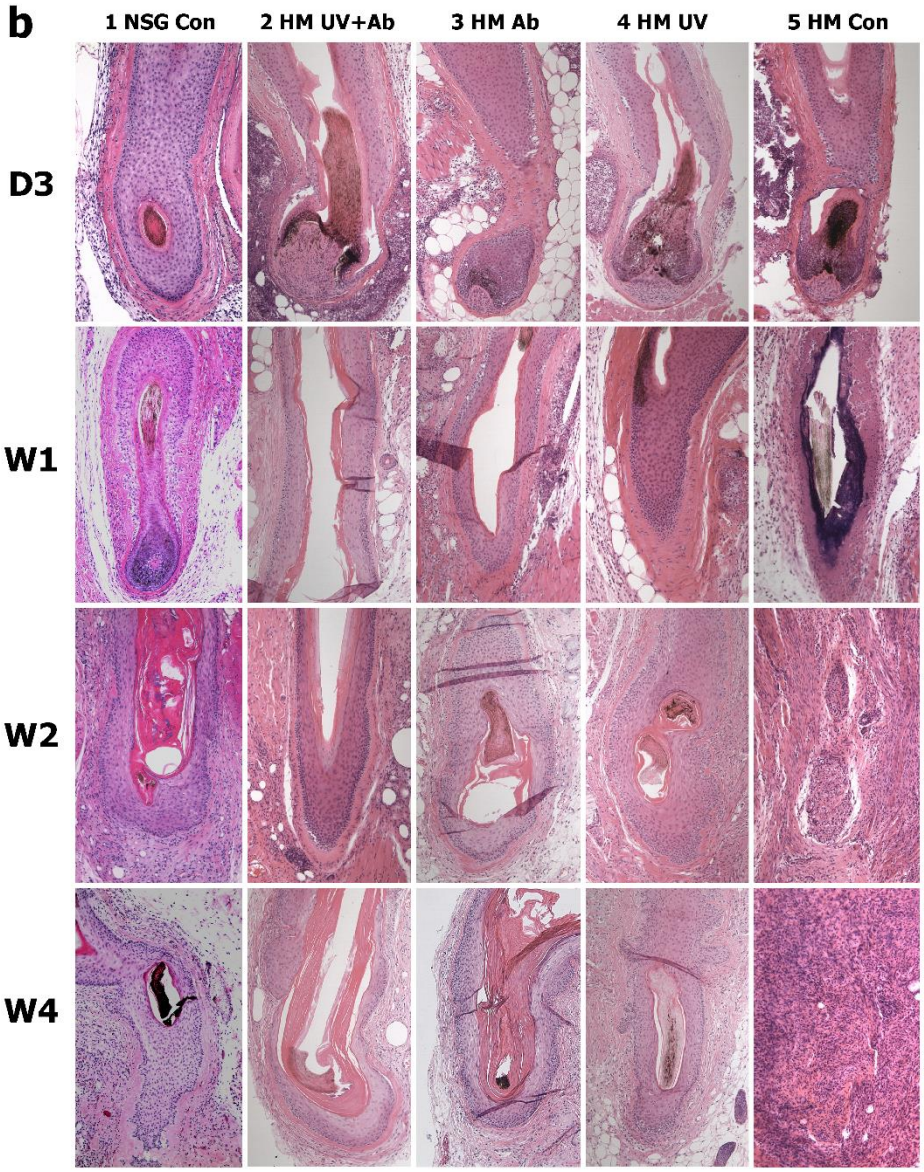

(b) Representative microscopic images from Group 1-5 at 3 days, 1 week, 2 weeks, and 4 weeks post-transplantation. At 1 week, the ORS in Group 2, 3, and 4 was maintained with an orderly structure, but the ORS in Group 5 started to get destroyed with perifollicular inflammation. At 4 weeks, the ORS was intact in Group 2, 3, and 4, whereas totally destroyed and replaced with granuloma in Group 5 (H&E, x100).

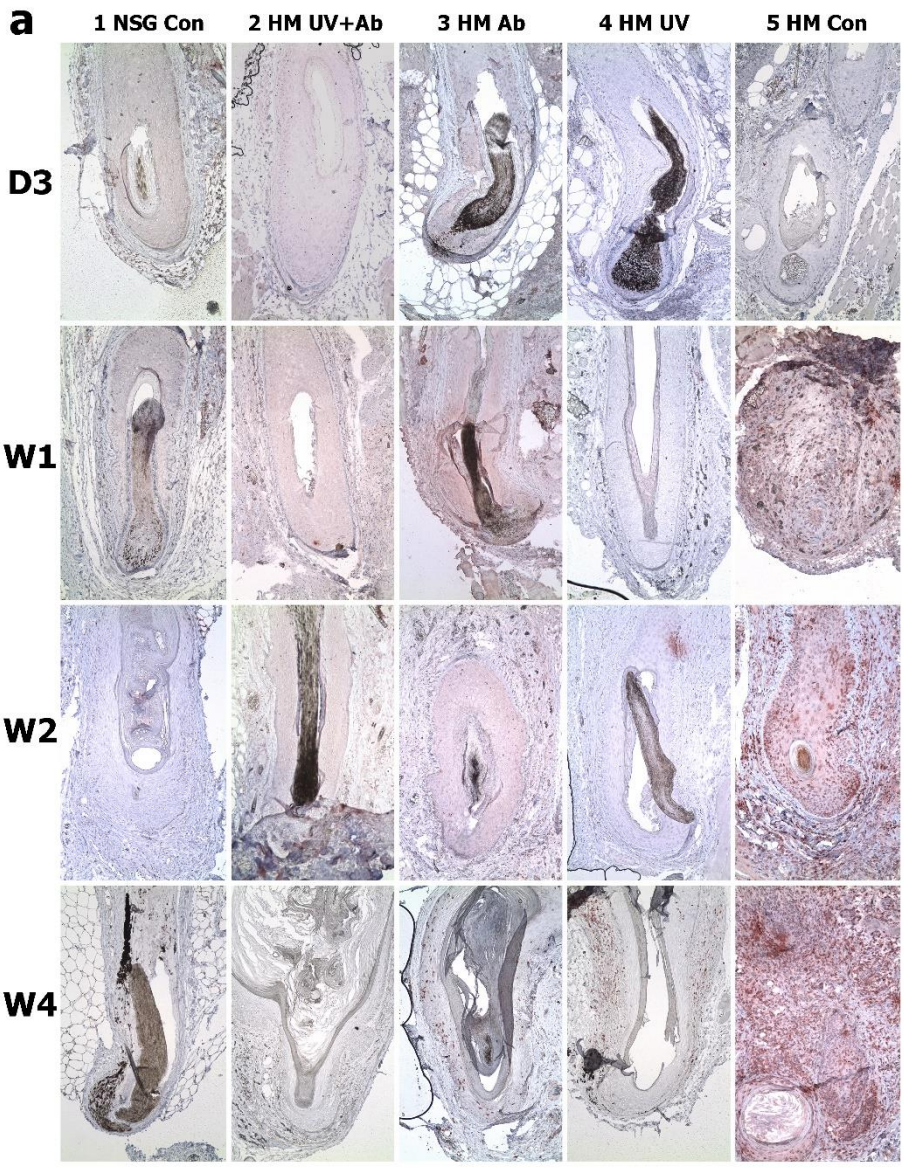
a
1 NSG Con
2 HM UV+Ab
3 HM Ab
4 HM UV
5 HM Con
D3
W1
W2
W4

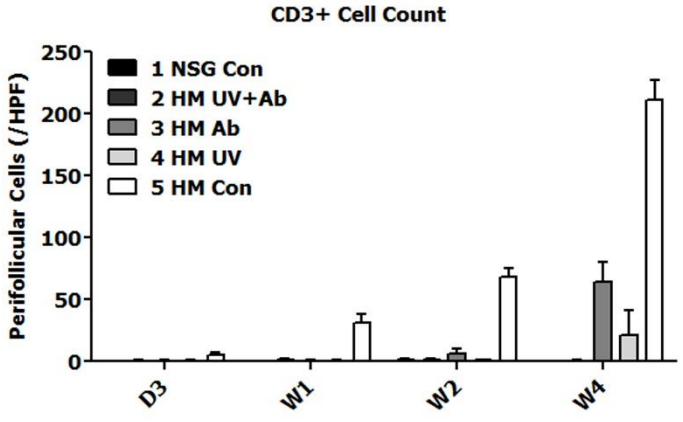
CD3+ Cell Count
Perifollicular Cells (/HPF)
250
200
150
100
50
0
1 NSG Con
2 HM UV+Ab
3 HM Ab
4 HM UV
5 HM Con
D3
W1
W2
W4

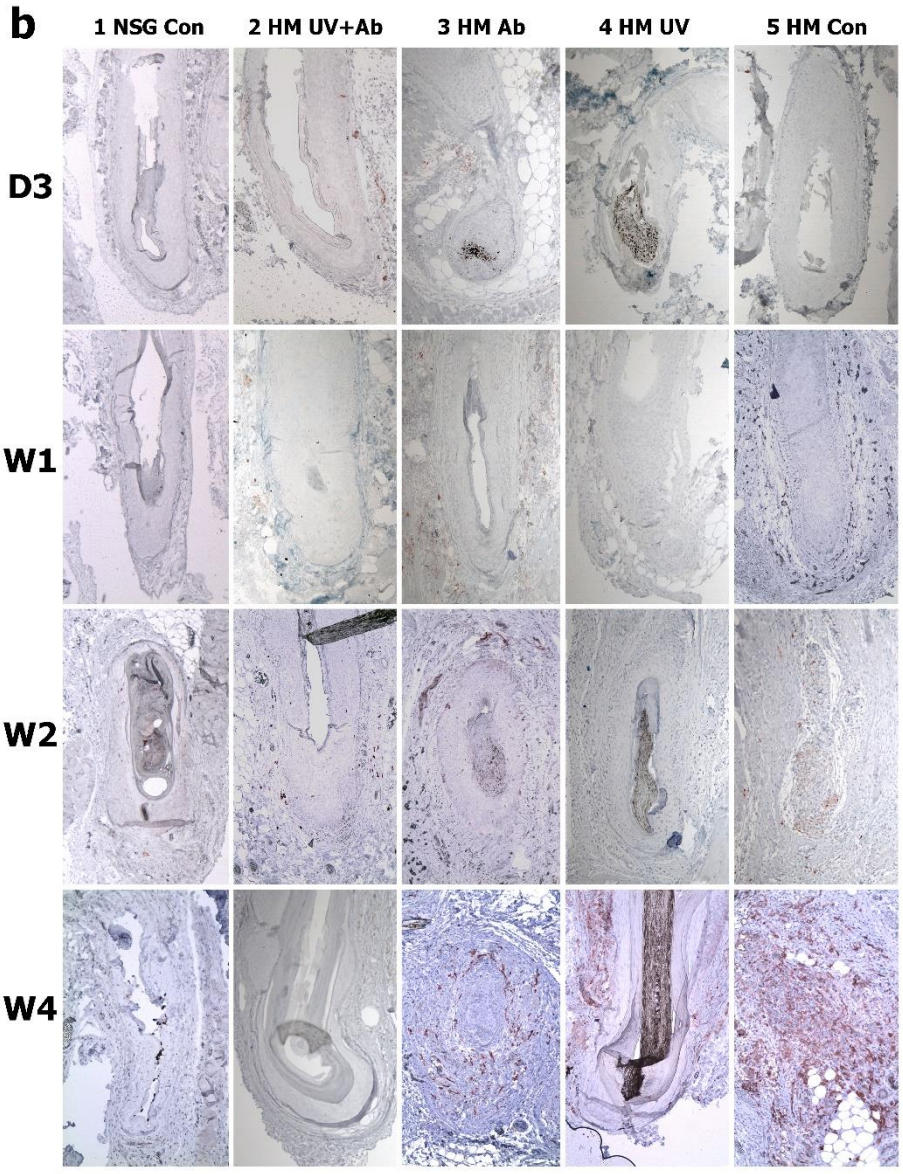
b
1 NSG Con
2 HM UV+Ab
3 HM Ab
4 HM UV
5 HM Con
D3
W1
W2
W4

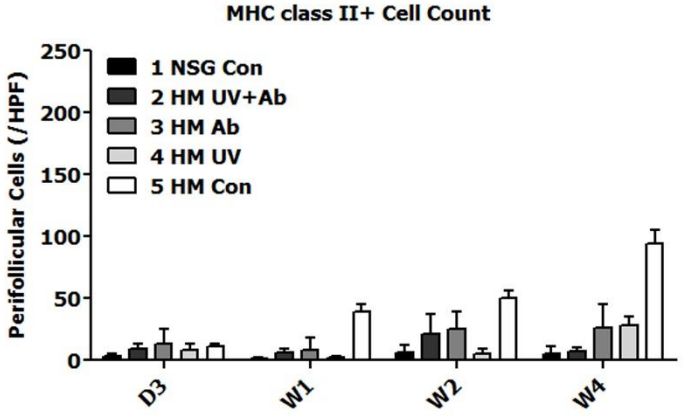
MHC class II+ Cell Count
Perifollicular Cells (/HPF)
250
200
150
100
50
0
1 NSG Con
2 HM UV+Ab
3 HM Ab
4 HM UV
5 HM Con
D3
W1
W2
W4

Figure 2-5. $CD3^+$ T cell and MHC class II^+ macrophage infiltration was diminished under UVB pre-irradiation and anti-CD154 antibody treatment.

Representative immunohistochemical images and quantification of perifollicular (a) $CD3^+$ T cells and (b) MHC class II^+ macrophages in Group 1-5 at 3 days, 1 week, 2 weeks, and 4 weeks post-transplantation. (3 fields/HF, 3-4 HFs/group, immunoperoxidase, x100).

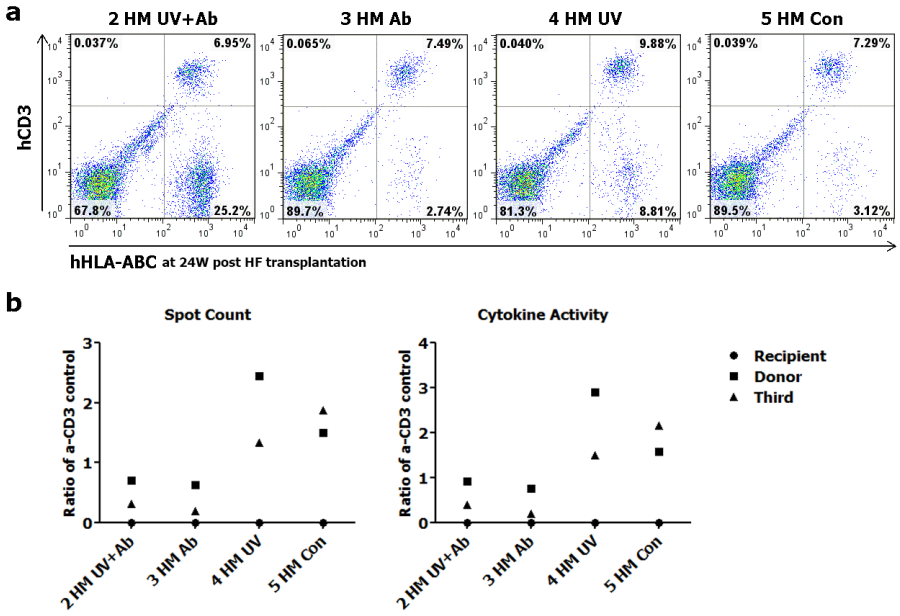

Figure 2-6. UVB pre-irradiation alone did not induce antigen-specific T cell tolerance.

(a) Representative flow cytometry plots of human HLA-ABC$^+$ cells in total splenocytes from humanized mice when they were sacrificed at 24 weeks post-transplantation. Human HLA-ABC$^+$ cells were still observed and well repopulated in total splenocytes of humanized mice (mean 7.90±0.67%). (b) Summarized data from ELISPOT assay to evaluate of IFN-γ-secreting T cells stimulated with none (recipient), donor PBMCs (donor), and third-party γ-irradiated human PBMCs (third), then normalized to anti-hCD3 antibody reactive T cells. The number of IFN-γ-secreting T cells was much lower in the Ab-treated Group 2 and 3 than the UV only-treated Group 4 (n=1 for each group).

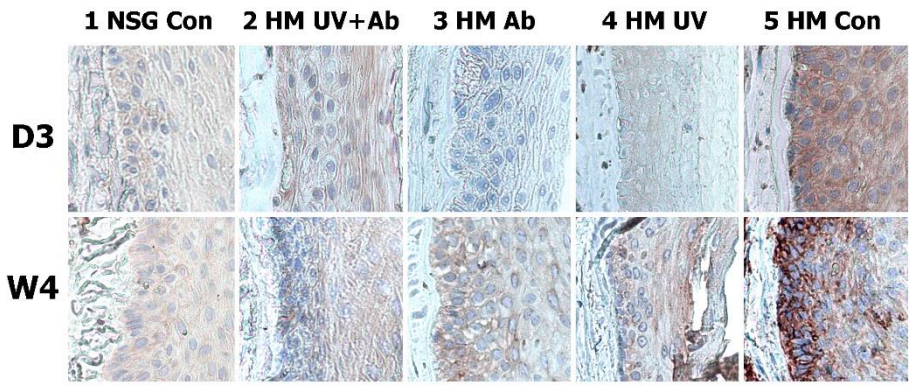

Figure 2-7. Immune privilege was maintained in surviving HF allografts.

Representative immunohistochemical images of MHC class I expression in the ORS of HF allografts in Group 1-5 at 3 days and 4 weeks post-transplantation (immunoperoxidase, x400).

DISCUSSION

During the past decade, numerous studies have unveiled the mechanisms of peripheral T cell tolerance mediated by DC subsets. Since the discovery of LFA-1/ICAM-1 interaction which plays a critical role in T cell-mediated immune responses, its potential as a therapeutic target has been evident [8, 27]. MD-3 antibody binds to the second domain of human and non-human primate ICAM-1 [8]. When DCs generated from monocytes in the presence of MD-3 were stimulated with lipopolysaccharide, they were not fully mature and arrested at the semi-mature stage in terms of low expression of MHC and co-stimulatory molecules and markedly decreased production of cytokines. Previously, MD-3 treatment in humanized mice which received porcine islet xenografts induced T cell tolerance against grafted antigens. Also, long-term xenograft survival was achieved in nonhuman primates when combined with low-dose rapamycin and anti-CD154 blocking antibody [8].

In the first part study, Cynomolgus monkeys received MD-3 antibody twice at 4 days and 1 day before transplantation. The survival of HF allografts was maintained under MD-3 treatment regardless of the concomitant immunosuppressant therapy. The hair shaft shedding was regarded as the phenomenon in which the growing shaft either pushes or pulls the resting hair shaft out. However, Milner Y *et al.* revealed that an active intercellular separation process is necessary in the shedding shaft base including a specific proteolytic step [28]. When the surrounding HF is

destroyed due to the proteolytic process, the central hair shaft is pulled out subsequently. Therefore, the number of hair shafts can be a useful indicator for graft survival within a short period of time. Consistently, we confirmed that the ORS of HF allografts was intact on histological examination before 4 weeks post-transplantation.

The arrival of T cell infiltrates was significantly delayed and their number was significantly lesser in MD-3-treated recipients compared with rapamycin only-treated and control recipients. During the inflammatory process, transendothelial T cell migration is dependent on LFA-1/ICAM-1 interaction, and thus there is a possibility that MD-3 treatment inhibited transendothelial T cell migration via blocking LFA-1/ICAM-1 interaction. However, considering a previous report which proved that leukocyte-endothelial adhesion was not affected by MD-3 treatment [8], this possibility is less likely. Regarding macrophages, heavy infiltration was found in the control group, while the number of infiltrated macrophages was not correlated with graft rejection in the MD-3 and rapamycin only treated groups. These findings suggest that T cell-mediated rejection was the major mechanism in HF allograft rejection, and MD-3 treatment was able to efficiently suppress T cell immunity. Consistently, DSAs were not developed in all three groups suggesting that HF allografts were not mainly affected by the humoral immune mechanism.

The skin immune system has evolved in the context of continuous exposure to a diverse microbiota or environmental challenges unlike the

visceral immune system [29]. DCs resident in the dermis egress via the afferent lymphatics to the lymph node where they directly present antigen to T cells [30]. Skin macrophages populate in the dermis, reside around the blood vessel, and can assist with the recruitment of neutrophils [31]. Lymphocytes are present in significant numbers in the dermis, in particular $CD4^+$ T cells [32]. The epidermal $CD8^+$ T cells persist for long periods within the epidermis, referred to as tissue-resident memory T cells. Therefore, in the skin as a reservoir of mature resident immune cells, MD-3 therapy may not enough to guarantee long-term survival of allografts. The final rejection would be mediated by antibodies against thymus-independent carbohydrate antigen, for example, mismatched ABO antigen, and activated macrophages [33].

Generally, T cell reaction is the rate-limiting step for allograft rejection as shown by indefinite allograft acceptance in α/β T cell receptor-deficient animal models [7]. In the first part, we illustrated that the major rejection of HF allograft was composed of cytotoxic $CD8^+$ T cells in skin immune system of nonhuman primate model [34]. Among alloreactive T cells, donor MHC-restricted T cells can be effectively activated with direct pathway by donor APCs and capable of a direct contact and donor MHC-dependent interaction with donor target cells [7]. And this donor APC-mediated T cell activation represents the driving force behind early acute graft rejection, which is very important in early post-transplantation period [35]. Therefore, by the successful depletion of donor APCs prior to transplantation, donor MHC-restricted recipient T cells

cannot be activated effectively, and also donor-reactive memory T cell formations can be avoided [36].

Recently, novel immunomodulatory strategies targeting T cell co-stimulatory pathways have gained considerable attention as a potential methods to control antigen-specific immune regulatory mechanisms [37]. CD154, also known as CD40 ligand, is constitutively expressed, and its expression further increased upon activation on APCs, including B cells, DCs and macrophages. It has been firmly established that CD40/CD154 co-stimulatory pathway plays a central role in T cell-mediated DC activation/maturation and macrophage activation [38]. Engagement of CD40 on these APCs stimulates the release of pro-inflammatory cytokines and chemokines, as well as CD28-mediated co-stimulation. However, antigen presentation by immature DCs results in T cell tolerance because of a failure to provide sufficient co-stimulatory signals [6]. Therefore, by using UVB pre-irradiation and anti-CD154 antibody, the dual blocking mechanisms were substantialized during the alloantigen presentation process by donor DCs or recipient DCs.

The HF is well recognized for its immune privilege, similarly to the anterior chamber of eye. The anagen stage of the HF is characterized by a conspicuous absence of MHC class I antigens and expression of potent immunosuppressants in the HF epithelium [39]. Cells of the immune system are also sparsely distributed in the HF so that only scant numbers of NK and T cells are found in the proximal HF and bulb [25]. NK cells readily kill MHC class I-negative cells, but there is no evidence of NK cell attack

to the normal HF epithelium [26]. This absence of NK cell-mediated injury is supposed to the result of the inhibitory effects two cytokines: macrophage migration inhibitory factor (MIF) and TGF-β2 [13, 26]. Normal human HFs maintain their immune privilege and escape the induction of autoimmune diseases like alopecia areata by reducing the chance of stimulation of NK cell activation [40-42]. However, in the autoimmune condition, cytotoxic immune response result in HF immune privilege collapsed showing the upregulation of MHC class I expression and downregulation of MIF molecule in the HF epithelium [13].

The most striking feature of the second part study is that several HF allografts survived showing normal hair cycle in the UV-only treated group. Previously, it has been reported that the depletion of donor-derived Langerhans cells by UV radiation promoted allograft survival in the corneal allograft model [43]. In our study, we observed the long-term survival of HF allografts by forcing donor DCs migrate out of donor HFs for the elimination of direct alloantigen presentation. Furthermore, HF immune privilege was maintained in this UV-only treated group. Therefore, the mechanism of immune privilege was supposed to be contributed to the HF allograft survival despite of lack of the recipient MHC class I molecule. In combination with the results of ELISPOT assay, the long-term survival of HF allografts in the UV-only treated group was not mediated by T cell tolerance, rather mediated by the evasion of immune surveillance likely to the normal HFs in vivo.

Traditionally, humanized mice referred to the mice engrafted with human cells or tissues [20]. These models have great advantages and interests to researcher who focused on translational research into clinical applications [14]. The humanized immune system by the engraftment of human HSCs into immunodeficient NSG mice is much more reliable in multilineage hematopoietic development and stable engraftment [44]. Human myeloid and plasmacytoid DCs are generated, as well as T and B cell populations and other human leukocyte subsets [44]. In this study, there were two important points for the generation of humanized mouse: the survival rate of adult NSG mice was not sufficient compared to wild-type mice and the success rate of human cell repopulation exhibited an individual variation among NSG mice.

Our HF allograft model is suitable for transplantation research, relatively easy to evaluate and more applicable, unlike solid organ transplantation. In the first part, we observed that MD-3 pretreatment considerably prolonged the HF allograft survival by diminishing alloreactive T cell infiltration. This attempt efficiently suppressed T cell response, but only targeted to the recipient immune system. In the second part, we observed that UVB pre-irradiation targeted the donor tissue achieved the long-term survival of HF allograft survival in humanized mouse model. In conclusion, a clinical application of allogeneic hair transplantation can be more possible by the new immunomodulatory strategy. The induction of antigen-specific T cell tolerance by MD-3 antibody or UVB pre-irradiation could be adopted in the skin immune

system and these strategies can be a potent immunomodulatory tool for preventing allograft rejection.

REFERENCES

1. Cash TF. The psychology of hair loss and its implications for patient care. *Clin Dermatol* **19**, 161–166 (2001).

2. Choi M*, et al.* Clinical characteristics of chemotherapy-induced alopecia in childhood. *J Am Acad Dermatol* **70**, 499–505 (2014).

3. Steinman RM, Hawiger D, Nussenzweig MC. Tolerogenic dendritic cells. *Annu Rev Immunol* **21**, 685–711 (2003).

4. Reis e Sousa C. Dendritic cells in a mature age. *Nat Rev Immunol* **6**, 476–483 (2006).

5. Morelli AE, Thomson AW. Tolerogenic dendritic cells and the quest for transplant tolerance. *Nat Rev Immunol* **7**, 610–621 (2007).

6. Shortman K, Naik SH. Steady-state and inflammatory dendritic-cell development. *Nat Rev Immunol* **7**, 19–30 (2007).

7. Lin CM, Gill RG. Direct and indirect allograft recognition: pathways dictating graft rejection mechanisms. *Curr Opin Organ Transplant* **21**, 40–44 (2016).

8. Jung KC, *et al.* In situ induction of dendritic cell-based T cell tolerance in humanized mice and nonhuman primates. *J Exp Med* **208**, 2477-2488 (2011).

9. Kolgen W, *et al.* Epidermal langerhans cell depletion after artificial ultraviolet B irradiation of human skin in vivo: apoptosis versus migration. *J Invest Dermatol* **118**, 812-817 (2002).

10. Duthie MS, Kimber I, Norval M. The effects of ultraviolet radiation on the human immune system. *Brit J Dermatol* **140**, 995-1009 (1999).

11. Racz E, *et al.* Effective Treatment of Psoriasis with Narrow-Band UVB Phototherapy Is Linked to Suppression of the IFN and Th17 Pathways. *J Invest Dermatol* **131**, 1547-1558 (2011).

12. Kwon OS, Kim MH, Park SH, Chung JH, Eun HC, Oh JK. Staged hair transplantation in cicatricial alopecia after carbon dioxide laser-assisted scar tissue remodeling. *Arch Dermatol* **143**, 457-460 (2007).

13. Ito T, *et al.* Maintenance of hair follicle immune privilege is linked to prevention of NK cell attack. *J Invest Dermatol* **128**, 1196-1206 (2008).

14. Pearson T, Greiner DL, Shultz LD. Creation of "humanized" mice to study human immunity. *Curr Protoc Immunol* Chapter 15, Unit 15 21 (2008).

15. Inagaki H. Morphological characteristics of the hair of Japanese monkeys (Macaca fuscata fuscata): Length, diameter and shape in cross-section, and arrangement of the medulla. *Primates* 27, 115-123 (1986).

16. Altshuler GB, Anderson RR, Manstein D, Zenzie HH, Smirnov MZ. Extended theory of selective photothermolysis. *Lasers Surg Med* 29, 416-432 (2001).

17. Miyasaka S, Yoshino M, Sato H, Miyake B, Seta S. The ABO blood grouping of a minute hair sample by the immunohistochemical technique. *Forensic Sci Int* 34, 85-98 (1987).

18. Lee DH, Jung JY, Oh JH, Lee S, Kim YK, Chung JH. Ultraviolet irradiation modulates ABO blood group antigens in human skin in vivo: possible implication in skin aging. *J Dermatol Sci* 66, 71-73 (2012).

19. Jensen EC. Quantitative analysis of histological staining and fluorescence using ImageJ. *Anat Rec (Hoboken)* **296**, 378-381 (2013).

20. Griffin RL, Kupper TS, Divito SJ. Humanized Mice in Dermatology Research. *J Invest Dermatol* **135**, e39-43 (2015).

21. Taguchi K, Fukunaga A, Ogura K, Nishigori C. The role of epidermal Langerhans cells in NB-UVB-induced immunosuppression. *Kobe J Med Sci* **59**, E1-9 (2013).

22. Okamoto H, Mizuno K, Itoh T, Tanaka K, Horio T. Evaluation of apoptotic cells induced by ultraviolet light B radiation in epidermal sheets stained by the TUNEL technique. *J Invest Dermatol* **113**, 802-807 (1999).

23. Schwarz T. Biological effects of UV radiation on keratinocytes and Langerhans cells. *Exp Dermatol* **14**, 788-789 (2005).

24. Braun S*, et al.* Keratinocyte growth factor protects epidermis and hair follicles from cell death induced by UV irradiation, chemotherapeutic or cytotoxic agents. *J Cell Sci* **119**, 4841-4849 (2006).

25. Christoph T, *et al.* The human hair follicle immune system: cellular composition and immune privilege. *Br J Dermatol* **142**, 862-873 (2000).

26. Niederkorn JY. Mechanisms of immune privilege in the eye and hair follicle. *J Investig Dermatol Symp Proc* **8**, 168-172 (2003).

27. Badell IR, *et al.* LFA-1-specific therapy prolongs allograft survival in rhesus macaques. *J Clin Invest* **120**, 4520-4531 (2010).

28. Milner Y, Sudnik J, Filippi M, Kizoulis M, Kashgarian M, Stenn K. Exogen, shedding phase of the hair growth cycle: characterization of a mouse model. *J Invest Dermatol* **119**, 639-644 (2002).

29. Naik S, *et al.* Commensal-dendritic-cell interaction specifies a unique protective skin immune signature. *Nature* **520**, 104-108 (2015).

30. Allan RS, *et al.* Migratory dendritic cells transfer antigen to a lymph node-resident dendritic cell population for efficient CTL priming. *Immunity* **25**, 153-162 (2006).

31. Abtin A, *et al.* Perivascular macrophages mediate neutrophil recruitment during bacterial skin infection. *Nat Immunol* **15**, 45-53 (2014).

32. Clark RA, *et al.* The vast majority of CLA+ T cells are resident in normal skin. *J Immunol* **176**, 4431-4439 (2006).

33. Takahashi K. A new concept of accommodation in ABO-incompatible kidney transplantation. *Clin Transplant* **19 Suppl 14**, 76-85 (2005).

34. Kim JY, *et al.* Allogeneic Hair Transplantation with Enhanced Survival by Anti-ICAM-1 Antibody with Short-Term Rapamycin Treatment in Nonhuman Primates. *J Invest Dermatol* **137**, 515-518 (2017).

35. Benichou G, Thomson AW. Direct versus indirect allorecognition pathways: on the right track. *Am J Transplant* **9**, 655-656 (2009).

36. Zhai Y, Meng L, Gao F, Busuttil RW, Kupiec-Weglinski JW. Allograft rejection by primed/memory CD8+ T cells is CD154 blockade resistant: therapeutic implications for sensitized transplant recipients. *J Immunol* **169**, 4667-4673 (2002).

37. Zhang T, Pierson RN, 3rd, Azimzadeh AM. Update on CD40 and CD154 blockade in transplant models. *Immunotherapy* **7**, 899-911 (2015).

38. Alaaeddine N, Hassan GS, Yacoub D, Mourad W. CD154: an immunoinflammatory mediator in systemic lupus erythematosus and rheumatoid arthritis. *Clin Dev Immunol* **2012**, 490148 (2012).

39. Paus R, Christoph T, Muller-Rover S. Immunology of the hair follicle: A short journey into terra incognita. *J Invest Derm Symp P* **4**, 226-234 (1999).

40. Boehm T. Quality control in self/nonself discrimination. *Cell* **125**, 845-858 (2006).

41. Paus R, Ito N, Takigawa M, Ito T. The hair follicle and immune privilege. *J Investig Dermatol Symp Proc* **8**, 188-194 (2003).

42. Gilhar A, Kalish RS. Alopecia areata: a tissue specific autoimmune disease of the hair follicle. *Autoimmun Rev* **5**, 64-69 (2006).

43. He YG, Niederkorn JY. Depletion of donor-derived Langerhans cells promotes corneal allograft survival. *Cornea* **15**, 82-89 (1996).

44. Shultz LD, Ishikawa F, Greiner DL. Humanized mice in translational biomedical research. *Nat Rev Immunol* **7**, 118-130 (2007).

국문초록

항원 특이적 면역 관용을 통한 동종간 모발이식술 개발

서울대학교 의과대학 의학과

피부과학전공 김진용

난치성 영구 탈모는 환자들에게 사회적, 정신적으로 큰 고통을 유발하기 때문에 반드시 치료가 필요하지만, 공여부로 이용할 수 있는 자가 모낭이 없는 경우 모발이식술의 대상이 될 수 없다. 하지만 항원 특이적 면역조절 기전을 통해서 동종간 모발이식술을 시행할 수 있다면, 난치성 영구 탈모 환자들에게 전신적 면역억제 없이 새로운 치료가 가능하다. 이를 위하여 장기이식 면역거부반응을 유도하는 핵심적인 세포로 주목받는 수지상세포를 대상으로 면역거부반응을 이해하고 새로운 조절 방법을 시도하였다. 구체적으로 항원제시과정에서 수지상세포의 성숙을 미성숙 상태로 중단시키거나, 공여 조직에 자외선을 조사하여 이미 존재하고 있는 조직 내 수지상세포를 미리 제거한 뒤, 영장류 모델 혹은 인간화마우스 모델에서 MHC class 가 서로 다른 개체 간 동종간 모발이식을 시행하였다. 이식한 모낭의 장기간 생존을 통하여 제시된 항원에 대해서만 선택적으로 면역관용 유도를 보여줌으로써, 이를 바탕으로 하는 동종간 모발이식술의 임상 적용에 대해 연구하였다.

첫번째 연구에서는 MD-3 항체를 이용하여 항원제시과정에서 수지상세포의 성숙을 중단시켜 면역관용을 유도하였다. 다이오드 제모 레이저를 이용하여 Cynomolgus monkey 의 등 부분의 피부에 조사하여,

모발이식을 위한 수여부를 확보하였다. 이후 MD-3 항체와 단기간 면역억제제의 복합 사용 하에 동종간 모발이식을 시행하고, 모낭 생착 여부를 임상적 평가 및 조직학적 검사를 통해 확인하였다. 면역억제제 단독군이나 대조군에 비해서 MD-3 사용군에서 이식 모낭의 생존이 수주 이상 유의하게 지속됨을 확인하였다. 또한 영장류의 말초혈액을 채취하여 각각의 공여-수여 개체 쌍에 따른 ELISPOT 검사 및 DSA 생성 검사로 하여 면역학적으로 항원특이적 면역관용 유도를 확인하였다.

후속 연구로 공여 모낭 조직에 자외선을 미리 조사하여 공여 조직 내에 존재하고 있는 조직 내 수지상세포를 제거한 뒤, 인간화마우스 모델에서 동종간 모발이식술을 시행하였다. 면역억제 NSG 마우스에 인간 제대혈 유래 $CD34^+$ 조혈모세포를 이식하여 인간화마우스를 제작하고, 사람 모낭을 분리하여 인간화마우스에 이식하였다. 이식할 사람 모낭에 생체 내, 생체 외 두 번의 UVB 를 조사하여 공여 모낭 내에 존재하고 있는 수지상세포를 제거하고, 이를 면역형광염색을 통해서 확인하였다. 인간화마우스에는 anti-CD154 항체를 투여하여 수여 개체 내의 항원제시기능을 억제하여 면역관용을 추가적으로 보조하였다. 이후 이식한 모낭이 6 개월 이상 생착하여 정상 모발 주기를 보이는 것을 확인하였다.

이를 통하여 항원 특이적으로 면역관용을 유도하는 가능성을 확인하고, MHC class 가 서로 다른 동종간 모발이식에서 새로운 면역조절 기전의 가능성을 제시하였다. 항원 특이적 면역관용 유도 기술의 확립을 통해 기존의 동종간 장기이식술에서 큰 한계점이던 장기간 전신적 면역억제제 투여를 최소화할 수 있고, 후천적으로 항원 특이적 면역관용을 유도해낼 수 있는 방법에 대해서 모색하였다. 모발이 풍부한 가족이나 자원자의 모낭을 이용하는 동종간 모발이식술을 통해 기존의 모발이식술의 한계점이었던

공여부 모낭부족 문제를 해결하고, 이를 임상에 적용하는 탈모치료법의 획기적인 발전 방법에 대해여 제시하였다.